JOURNAL OF VIROLOGY, Jan. 1997, p. 291–298
0022-538X/97/$04.00+0

Vol. 71, No. 1

Genetic Analysis of the Yellow Fever Virus NS1 Protein: Identification of a Temperature-Sensitive Mutation Which Blocks RNA Accumulation

ISABELLA R. MUYLAERT,[1] RICARDO GALLER,[2] AND CHARLES M. RICE[1]*

Department of Molecular Microbiology, Washington University School of Medicine, St. Louis, Missouri 63110-1093,[1] *and Departamento de Bioquímica e Biologia Molecular, Fundação Oswaldo Cruz, Rio de Janeiro 21040, Brazil*[2]

Received 2 August 1996/Accepted 27 September 1996

The flavivirus NS1 protein is a highly conserved nonstructural glycoprotein that is capable of eliciting protective immunity. NS1 homodimers are secreted from virus-infected mammalian cells, but the protein is also present at the plasma membrane and in the lumen of intracellular vesicles. Based on these properties, it has been speculated that NS1 may function in virus maturation or release. To gain further insight into NS1 function, we used clustered charged-amino-acid-to-alanine mutagenesis to create 28 clustered substitutions in the NS1 protein of yellow fever virus. To screen for conditional mutations, full-length RNAs containing each mutation were assayed for plaque formation at 32 and 39°C after RNA transfection. We found that 9 mutations were lethal, 18 allowed plaque formation at both temperatures, and 1, *ts*25, was strongly heat sensitive and was unable to form plaques at 39°C. Lethal mutations clustered in the amino-terminal half of NS1, whereas those leading to impaired replication relative to the parent were distributed throughout the protein. High-multiplicity infections at 39°C demonstrated that *ts*25 was defective for RNA accumulation, leading to depressed viral protein synthesis and delayed virus production. Although *ts*25 secreted less NS1 than did the parent, temperature shift experiments failed to demonstrate any temperature-dependent differences in polyprotein processing, NS1 stability and secretion, or release of infectious virus. The *ts* lesion of *ts*25 was shown to be due to a single alanine substitution for Arg-299, a residue which is conserved among flaviviruses. These results argue that NS1 plays an essential but as yet undefined role in flavivirus RNA amplification.

Flaviviruses are small, enveloped, positive-strand RNA viruses belonging to the family *Flaviviridae* (see references 3, 5, 31, 38, and 52 for reviews). Members of the *Flavivirus* genus are typically arthropod borne, being transmitted to vertebrates by infected mosquito or tick vectors; a number of them cause significant human morbidity and mortality worldwide (31). The genome RNA of yellow fever virus (YFV), the prototype member of this genus, is 10,862 bases long and contains a 5′ cap and a nonhomopolymeric 3′-terminal stem-loop structure (40). The incoming genome RNA is translated as a large polyprotein, which is cleaved by host and viral proteases to produce the mature structural and nonstructural (NS) proteins (5, 42). The protein order in the polyprotein is NH_2-C-prM(M)-E-NS1-NS2A-NS2B-NS3-NS4A-2K-NS4B-NS5-COOH, where C (capsid), prM(M) (membrane), and E (envelope) represent the structural proteins or their precursors and NS1 through NS5 are NS proteins (5, 26, 42).

Flavivirus RNA replication, a membrane-associated event, occurs in the cytoplasm via a negative-strand intermediate and is asymmetric, leading to the preferential accumulation of positive-strand RNAs (5, 52). Several NS proteins have been implicated in this process. The NS2B-3 serine proteinase is required for processing at multiple sites in the NS polyprotein; these cleavages are presumably important for assembly of functional replication complexes (8, 9, 33). NS3 also possesses RNA-stimulated nucleoside triphosphatase (49), RNA helicase (11), and RNA triphosphatase activities (50). The N-terminal domain of NS5 contains sequence elements characteristic of methyltransferases (23), as well as a GDD motif, which is common to many viral RNA-dependent RNA polymerases (RDRP) (21). RDRP activity has been demonstrated for NS5 expressed in *Escherichia coli* (48), and recent work has shown that NS5 is phosphorylated on serine residues (22). Enzymatic functions for the remaining NS proteins have not been determined, but the smaller hydrophobic proteins NS2A, NS4A, and NS4B may play structural roles in replicase assembly or mediate interaction of other replicase components with host cell membranes (52).

The remaining NS protein, NS1, is a highly conserved glycoprotein containing 12 invariant cysteine residues and two potential N-linked glycosylation sites (5). NS1 is inserted into the endoplasmic reticulum lumen via a signal sequence located near the C terminus of the E protein and produced by cleavage of a discrete NS1-2A precursor (6). Dimerization occurs shortly after synthesis, and NS1 is present in intracellular, cell surface, and secreted forms (29, 53, 54). NS1 does not contain obvious membrane-spanning segments, and the mechanism by which it associates with cellular membranes is unknown. Interestingly, immunization with NS1 or passive transfer of NS1-specific antibodies can confer protective immunity against flavivirus infection (17, 19, 20, 44, 46, 47). Based on these properties, it was originally proposed that NS1 might play a role in viral assembly and/or maturation (29, 41). However, recent immunolocalization studies of dengue 2 virus (DEN2) NS1 (28), as well as our analysis of YFV NS1 glycosylation mutants (32), suggest the possible involvement of NS1 in viral RNA replication.

For many biological systems, conditional mutants have proven invaluable in studying protein function. For flaviviruses, temperature-sensitive (*ts*) mutants with defects in viral adsorption (15), RNA accumulation, and virulence have been isolated but only partially characterized (3). In this study, 28 YFV NS1 mutants were generated by clustered charged-ami-

* Corresponding author. Phone: (314) 362-2842. Fax: (314) 362-1232.

no-acid-to-alanine scanning mutagenesis (12, 51) and one strongly *ts* mutant (*ts*25) was obtained. Phenotypic analysis of these mutants provides a preliminary genetic map of NS1 functional domains, and characterization of *ts*25 argues strongly that NS1 is required for efficient amplification of flavivirus RNA.

MATERIALS AND METHODS

Cell cultures, virus stocks, and plaque assay. SW-13 cells were propagated in alpha minimal essential medium (αMEM) supplemented with 10% fetal calf serum (FCS). To prepare high-titer virus stocks, subconfluent monolayers of SW-13 cells (in 150-mm dishes) were infected at a multiplicity of infection (MOI) of 0.01 PFU of the parental virus (YFiv5.2) or temperature-sensitive mutant *ts*25 (both recovered from RNA transfection supernatants [see below]) per cell. After incubation for 3 days at 32°C in αMEM–2% FCS, culture supernatants were harvested, clarified at 3,000 × *g* for 10 min, aliquoted, and stored at −80°C. Titers of virus stocks were determined by plaque assay on SW-13 cells at 32 or 39°C (32). Plaques were visualized after 4 or 5 days by staining with 0.02% neutral red in phosphate-buffered saline (PBS) and, after fixation of the cells with 7% formaldehyde, with 1.3% crystal violet in 20% ethanol.

Plasmid constructions and site-directed mutagenesis. DNA manipulations were performed by standard methods (1, 43). Clustered charged-amino-acid-to-alanine and single mutations (see Table 1) were made by oligonucleotide-directed mutagenesis with uridylated (24, 27) phagemid pH2J1-NS1/2A DNA (32). To facilitate the construction of full-length templates containing the NS1 mutations, the plasmid pYFM5.2/15 was created by digesting pYFM5.2 (39) with *Avr*II and *Bgl*II, filling in the protruding ends, and religation. Mutagenized sequences were subcloned into pYFM5.2/15 by replacing the corresponding *Sst*I-*Bam*HI (for mutants A2 to A9, A30, and A31), *Sst*I-*Mlu*I (for mutant A10), *Bam*HI-*Mlu*I (for mutants A11 to A16), *Bam*HI-*Kpn*I (for mutant A17), *Mlu*I-*Kpn*I (for mutants A18 to A22), and *Kpn*I-*Pvu*II (for mutants A23 to A29, A32 and A33) fragments. For all constructs, the sequence of the entire subcloned fragment was confirmed. Mutant pYFM5.2 derivatives were constructed by replacement of the *Sse*8387I-*Avr*II fragment pYFM5.2 with the corresponding fragment from the mutant pYFM5.2/15 derivatives. Full-length YF 17D cDNA templates were constructed by in vitro ligation of restriction fragments from pYF5′3′IV and pYFM5.2 or its mutant derivatives (39).

In vitro transcription and RNA transfection. 5′-capped transcripts were synthesized in vitro from ligated cDNA templates by using SP6 RNA polymerase (39). Trace quantities of [^{3}H]UTP were included in the transcription reaction mixtures to allow quantitation and gel analysis of the RNA transcripts. Incorporation was measured by adsorption to DE81 (Whatman) filter paper (43). Subconfluent SW-13 monolayers (35-mm dishes) were used for RNA transfection with Lipofectin (GIBCO-BRL) (39), and transfection was performed, simultaneously, at 32 and 39°C to allow the direct identification of *ts* mutants. Briefly, transfection mixtures were made by adding 200 ng of each RNA transcript to 400 μl of PBS containing 16 μl of Lipofectin and incubating the mixture on ice for 10 min. Half this mixture was added to each of two cell culture dishes and incubated at room temperature for 10 min. Transfected monolayers were washed once with αMEM, and one set was incubated with αMEM–2% FCS for 3 days at 32 or 39°C. Culture fluids were harvested, clarified by centrifugation at 3,000 × *g* for 10 min, aliquoted, and stored at −80°C. Viral titers were determined by plaque assay at 32 or 39°C, as described above. The parallel set of transfected plates was overlaid with agarose (32) and assayed directly for plaque formation at 32 or 39°C.

Virus growth analyses. To measure virus production at constant temperatures, subconfluent monolayers of SW-13 cells (in 35-mm dishes) were infected at a MOI of 5 PFU of the parental virus or *ts*25 per cell in αMEM–2% FCS. After a 1-h incubation at 32 or 39°C, the inoculum was removed and the monolayers were washed with prewarmed αMEM and incubated with 2 ml of αMEM–2% FCS. Differential growth curves were generated by harvesting and replacing the culture supernatants at 12, 24, 48, or 72 h postinfection (p.i.). Aliquots were stored at −80°C, and titers were determined by plaque assay on SW-13 monolayers at 32 and 39°C.

To measure virus release upon temperature shift-up, subconfluent monolayers of SW-13 were infected with the wild-type virus or *ts*25 at 32°C, as described above. At 45 h p.i., the cells were washed with prewarmed αMEM, the medium was replaced with fresh medium, and incubation was continued at either 32 or 39°C. After 3 h, culture supernatants were harvested and stored at −80°C, and released viral titers were determined by plaque assay at 32 and 39°C.

Analysis of viral proteins. SW-13 monolayers (in 35-mm dishes) were infected at a MOI of 5 PFU of the wild-type virus or *ts*25 per cell and incubated at 32 and 39°C (both adsorption and incubation were done at these temperatures). At 36 h p.i., the cells were labeled at these temperatures for 6 h in methionine-free αMEM–2% FCS containing 40 μCi of Tran-^{35}S label (ICN) per ml. For pulse-chase experiments, cells were infected as described above at 32°C. At 35 h p.i., the cells were labeled for 1 h at either 32 or 39°C in methionine-free αMEM–2% FCS–100 μCi of Tran-^{35}S label per ml and either harvested immediately or incubated at 32 or 39°C for an additional 6 h in αMEM–2% FCS containing 10 times the normal amount of unlabeled methionine. At the indicated times, supernatants were collected and clarified by centrifugation at 3,000 × *g* for 2 min and monolayers were lysed in either sodium dodecyl sulfate (SDS)- or Triton X-100 containing lysis solution, as described previously (7). Triton X-100-treated proteins were immunoprecipitated with a YFV 17D-specific mouse hyperimmune ascitic fluid, and SDS-treated viral proteins were immunoprecipitated with a combination of NS1-specific rabbit polyclonal antibody (6) and mouse monoclonal antibodies 8G4 and 1A5 (45), as previously described (7). Immunoprecipitates were collected with *Staphylococcus aureus* Cowan 1 (Calbiochem) and separated by SDS-polyacrylamide gel electrophoresis (PAGE) (7, 25). The gels were treated with 1 M sodium salicylate (pH 7.0) for fluorographic detection of radiolabeled proteins at −80°C (4).

RNA analysis. To measure RNA accumulation during continuous incubation at 32 or 39°C, SW-13 monolayers (in 35-mm dishes) were infected at these temperatures with a MOI of 5 PFU of the wild-type virus or *ts*25 per cell and incubated for 36 h. In shift-up analyses, SW-13 cells were infected and incubated at 32°C for 18 h followed by an additional 18 h at either 32 or 39°C. To harvest RNA, the cells were washed once with ice-cold PBS and total cellular RNA was isolated by the RNAzol method (TEL-TEST, Inc.). A one-cycle or two-cycle RNase protection assay (32, 34) was used for analysis of positive- and negative-strand YFV RNAs, respectively. ^{32}P- or ^{35}S-labeled positive- or negative-sense RNA probes, encompassing the region of the YFV genome between nucleotides (nt) 3839 and 4089, were produced by in vitro transcription. Probe and protected RNAs were 284 and 251 nt, respectively. Protected RNAs were analyzed by electrophoresis in a 5% polyacrylamide–urea gel (43), and the bands were quantified with a phosphorimaging system (Bio-Rad).

RESULTS

In a previous study, we showed that ablation of the first or both YFV NS1 N-glycosylation sites led to impaired RNA accumulation, slow virus production, and decreased mouse neurovirulence (32). Since these glycosylation mutations were not conditional, it was not possible to precisely define the step(s) in YFV replication affected by these NS1 defects. To continue our genetic analysis of NS1 function, clustered charged-amino-acid-to-alanine mutagenesis (12, 51) was used to create a new panel of 28 YFV NS1 mutants (Table 1). For both yeast actin (51) and the poliovirus RDRP (12), this method has produced a number of useful conditional mutants. Clusters of two charged residues in a window of 5 amino acids in the NS1 coding region were replaced with alanine residues, as described by Wertman et al. (51). Since the sensitivity of NS1 to mutagenesis was unknown, both highly conserved and nonconserved charged residues were targeted.

Phenotypic characterization of clustered charged-amino-acid-to-alanine NS1 mutants. SW-13 monolayers were transfected with the parent or the clustered charged-amino-acid-to-alanine mutant RNAs followed by incubation at either 32 or 39°C. These two temperatures were chosen based on preliminary experiments examining plaque formation and virus yield at various temperatures (data not shown). Parallel samples were overlaid with agarose or incubated with medium to assay, respectively, for plaque formation and release of infectious virus. For the parent (YFiv5.2), transcript RNA specific infectivity and the titer of released virus titer (at 72 h) were approximately 2- and 10-fold lower, respectively, at 39°C than at 32°C. The lower yield of parental virus at 39°C is probably due to the shorter growth cycle observed at this temperature (see below) and increased thermal inactivation of the virus at the higher temperature. In any case, 19 of the 28 mutant RNAs produced plaques at both temperatures with specific infectivities similar to those of the parental transcripts (Table 1). Five of them (A5, A10, A15, A18, and A29) were phenotypically similar to the parent in terms of plaque size and released-virus titers. Thirteen mutants (A6, A8, A12, A16, A19, A20, A21, A22, A23, A24, A26, A27, and A28) exhibited smaller plaque phenotypes and/or reduced virus yields compared to the parent. A single mutant (A25) was strongly *ts*, exhibiting no plaque formation and limited virus production at 39°C (Table 1; see below). No plaques were observed at either temperature for nine of the mutant RNAs (A2, A3, A4, A7, A9, A13, A17, A30, and A31).

TABLE 1. Summary of YFV NS1 mutations and mutant phenotypes

Virus[a]	NS1 amino acid residue(s) changed to alanine	RNA specific infectivity[b] at:		Virus titer[c] at:		Plaque morphology[d] at:	
		32°C	39°C	32°C	39°C	32°C	39°C
wt	None	55	25	8.0×10^7	7.5×10^6	L	L
A2	K-14, D-17	0	0	≤50	≤50	—	—
A3	R-23, D-24	0	0	≤50	≤50	—	—
A4	D-27, K-31	0	0	≤50	≤50	—	—
A5	D-38, K-41	52	26	3.0×10^7	1.0×10^7	L	L
A6	E-51, E-52	53	29	1.5×10^7	6.5×10^6	S	S
A7	D-61, E-64	0	0	≤50	≤50	—	—
A8	R-69, R-71	26	10	2.0×10^5	1.0×10^5	S	S
A9	E-83, D-85	0	0	≤50	≤50	—	—
A10	D-92, K-94	70	31	5.0×10^7	4.0×10^6	L	L
A12	K-116, K-120	30	17	1.5×10^6	3.0×10^6	M	M
A13	R-128, K-129	0	0	≤50	≤50	—	—
A15	K-141, E-142	55	31	6.4×10^7	2.5×10^6	L	L
A16	E-156, E-157	30	15	1.5×10^6	3.0×10^6	M	M
A17	R-166, D-170	0	0	≤50	≤50	—	—
A18	D-178, D-180	51	25	3.0×10^7	1.5×10^6	L	L
A19	K-191, K-192	13	7	1.1×10^6	4.5×10^6	M	M
A20	E-217, D-220	31	19	7.0×10^3	5.0×10^2	S	S
A21	E-223, E-225	30	17	3.5×10^6	4.0×10^6	M	M
A22	E-238, E-240	33	19	1.5×10^7	2.1×10^7	M	M
A23	E-274, K-276	50	33	4.8×10^7	7.5×10^6	M	M
A24	D-288, D-292	45	17	2.5×10^7	3.0×10^6	M	M
A25	K-296, R-299	50	0	1.0×10^7	≤50	S	—
A26	D-303, K-306	50	20	1.3×10^6	5.0×10^6	S	S
A27	E-310, R-314	52	32	4.5×10^7	5.0×10^6	M	M
A28	E-334, R-336	48	21	4.5×10^6	7.5×10^5	S	S
A29	K-339, E-342	45	24	5.5×10^7	2.8×10^6	L	L
A30	D-73, E-74	0	0	≤50	≤50	—	—
A31	E-80, E-81	0	0	≤50	≤50	—	—
A32	K-296	56	31	6.5×10^7	4.0×10^6	L	L
A33	R-299	52	0	1.3×10^7	≤50	S	—

[a] wt, parental virus.
[b] Number of plaques obtained at 32 or 39°C after transfection of SW-13 monolayers with 20 ng of transcript RNA (see Materials and Methods). Plaques were stained and counted at 4 or 5 days posttransfection.
[c] Viral titer (PFU per milliliter) in the medium at 72 h posttransfection. After transfection, SW-13 monolayers were incubated at either 32 or 39°C. Plaque assay mixtures were incubated at the same temperature used to rescue the virus.
[d] Relative plaque size (L, large; M, medium; S, small) or no plaques detected (—).

Since the principal goal of this work was to obtain and study conditional NS1 mutants, we focused on characterization of the strongly *ts* mutant A25 (designated *ts*25). For subsequent studies, high-titer *ts*25 stocks were obtained after one passage in SW-13 monolayers at 32°C; no phenotypic reversion was observed as shown by the absence of plaque-forming virus at 39°C (data not shown).

The growth of *ts*25 is severely restricted at 39°C. As an initial step toward characterizing the conditional defect(s) of *ts*25, we examined the production of infectious virus during constant-temperature infections at either 32 or 39°C. SW-13 cells were infected at a high MOI with the parental virus or *ts*25, and titers of virus released during 0 to 12, 12 to 24, 24 to 48, and 48 to 72 h p.i. were determined by plaque assay at 32°C (Fig. 1). At 32°C, the permissive temperature, *ts*25 replicated to comparable levels and induced similar cytopathic effects (CPE) as compared to the parental virus, although the growth was slightly delayed. However, at 39°C, the nonpermissive temperature, *ts*25 growth was dramatically delayed as evidenced by severely reduced virus accumulation and little or no observable CPE, even after 72 h. In contrast, the parental virus produced strong CPE and high virus yields, peaking at 24 to 48 h p.i. To assay for possible *ts*25 revertants, titers were also determined at 39°C. No plaques were observed at 39°C for *ts*25 produced at either temperature, indicating that progeny produced at 39°C did not represent the emergence of wild-type revertants or pseudorevertants. These results suggest that the replication of *ts*25 is severely impaired at 39°C. However, the defect appears to be leaky, since low levels of virus are produced after prolonged incubation at the nonpermissive temperature.

The *ts*25 lesion leads to reduced accumulation of YFV-specific proteins at 39°C. To investigate whether the block in virus production correlated with reduced viral protein synthesis, we examined protein accumulation during constant-temperature infections. SW-13 cells were infected at a high MOI with the parental virus or *ts*25 at 32 and 39°C and were metabolically labeled, and YFV-specific proteins were immunoprecipitated and separated by SDS-PAGE (Fig. 2A). Except for reduced amounts of NS1, the level and profile of virus-specific proteins observed at 32°C were similar for *ts*25 and the parental virus. However, at 39°C, although the pattern was essentially the same for the parental virus, YFV-specific proteins were not detected in cells infected with *ts*25.

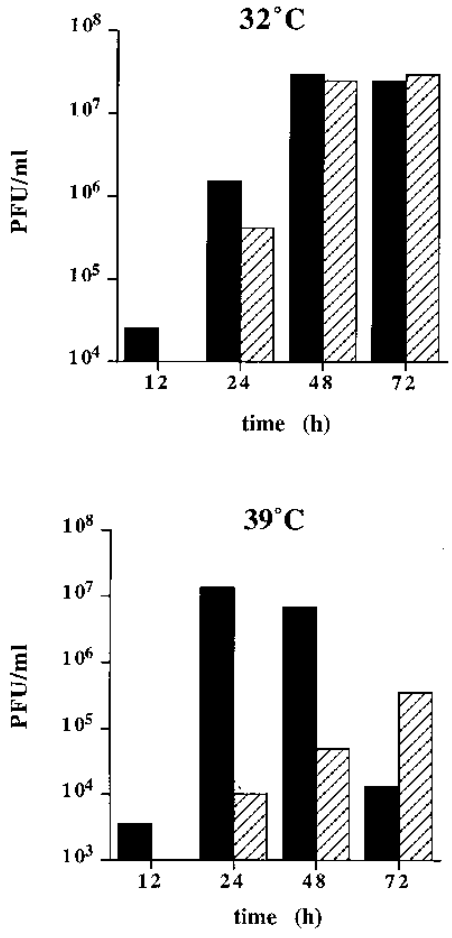

FIG. 1. Growth of *ts*25 and the parental virus at 32 and 39°C. SW-13 cells were infected at a MOI of 5 PFU of either the parental wild-type virus (solid bars) or *ts*25 (hatched bars) per cell at 32°C (the permissive temperature) or 39°C (the nonpermissive temperature). At 12 h p.i., the medium was harvested and replaced with fresh medium. This was repeated at 24, 48, and 72 h p.i. The titer of virus released during each time interval was determined by plaque assay on SW-13 cells at 32°C.

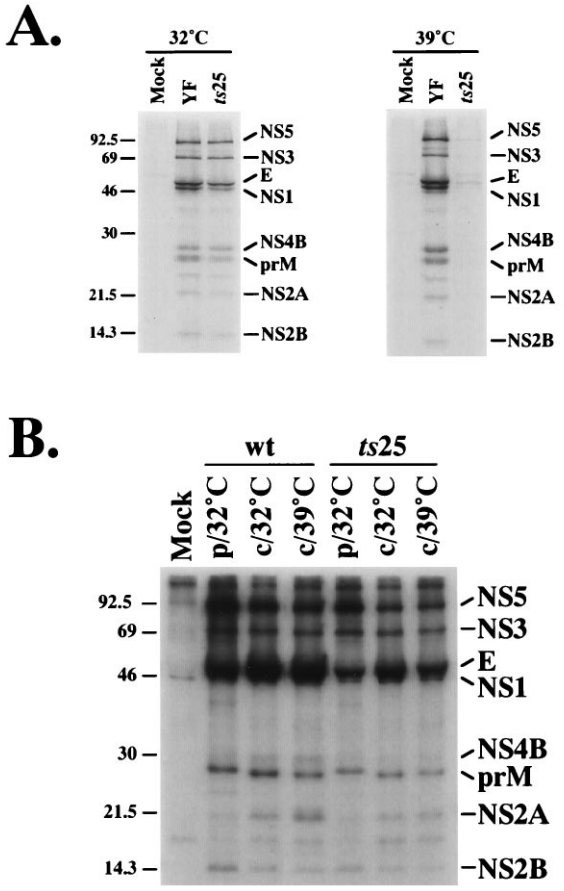

FIG. 2. Viral protein synthesis. (A) SW-13 cells were mock infected or infected at a MOI of 5 PFU of either the wild-type parent (wt) or *ts*25 per cell, incubated at 32 or 39°C for 36 h, and metabolically labeled at these temperatures for 6 h. (B) SW-13 cells were infected and incubated at 32°C for 35 h, pulse-labeled for 1 h (p), and chased (c) for 6 h at either 32 or 39°C. Cell extracts were immunoprecipitated with YFV-specific hyperimmune ascitic fluid and analyzed by SDS-PAGE (13% polyacrylamide). Molecular mass markers (in kilodaltons) are indicated on the left; YFV-specific proteins are indicated on the right.

***ts*25 exhibits an early defect in RNA accumulation.** The simplest explanation for the lack of virus-specific protein synthesis in *ts*25-infected cells at 39°C is that the lesion led to impaired RNA amplification and reduced levels of genome-length viral mRNA. To examine this possibility, SW-13 cells were infected at a high MOI with the parental virus or *ts*25 at 32 or 39°C for 36 h and accumulation of positive- and negative-strand RNAs was analyzed by an RNase protection assay. At 32°C, the permissive temperature, the levels of positive- and negative-strand RNAs in *ts*25-infected cells were approximately twofold lower than those of the parental virus (Fig. 3A). In contrast, at 39°C, *ts*25 RNA synthesis was not readily detected above background (Fig. 3A). Although a band of the expected size for a fragment protected by positive-strand RNA can be seen for *ts*25 at 39°C, similar levels of this product were also observed when RNA from mock-infected cells was used.

Nature of the *ts*25 RNA defect. We next examined the effect of a temperature shift on RNA accumulation. In this experiment, monolayers were infected at 32°C, as described above, and at 18 h, incubations were either continued at 32°C or shifted to 39°C for an additional 18 h. RNA accumulation was again determined by an RNase protection assay (Fig. 3B) and quantified with a phosphorimager (data not shown). For the parental virus, the levels of both positive- and negative-strand RNAs after the shift to 39°C were approximately twofold higher when compared to those produced by continuous incubation at 32°C (Fig. 3B). After 18 h, the molar ratio of positive-strand to negative-strand RNA was approximately 10; by 36 h, this ratio was 40 (39°C) or 50 (32°C). These data suggest that the asymmetry in positive- and negative-strand RNA synthesis increases during the course of infection. For *ts*25, the level of negative-strand RNA at 18 h was similar to that of the parent but increased only twofold after the shift to 39°C (in contrast to the eightfold increase observed at 32°C). These data suggest a heat-sensitive defect in *ts*25 negative-strand RNA accumulation. Relative to the parent, positive-strand RNA accumulation was also reduced for *ts*25 at both 32 and 39°C. After 18 h at 32°C, the molar ratio of positive- to negative-strand RNA was only 3 (as compared to ~10 for the parent). By 36 h at 32°C, this ratio had increased to about 35 (as compared to ~50 for the parent). In the shift-up experiment, a 10-fold increase in positive-strand RNA accumulation was observed for *ts*25, corresponding to a molar ratio of positive- to negative-strand RNA of 14. Thus, at 32°C, *ts*25 replicates more slowly than the parent, accumulating lower levels of both negative- and positive-strand RNAs. If the cells are shifted to 39°C, the *ts*25 defect is more dramatic, resulting in little additional accumulation of negative-strand template RNA and reduced accumulation of positive-strand RNA. It is clear, however, that once infection is established at 32°C, RNA synthesis can continue after the shift to the nonpermissive temperature. This conclu-

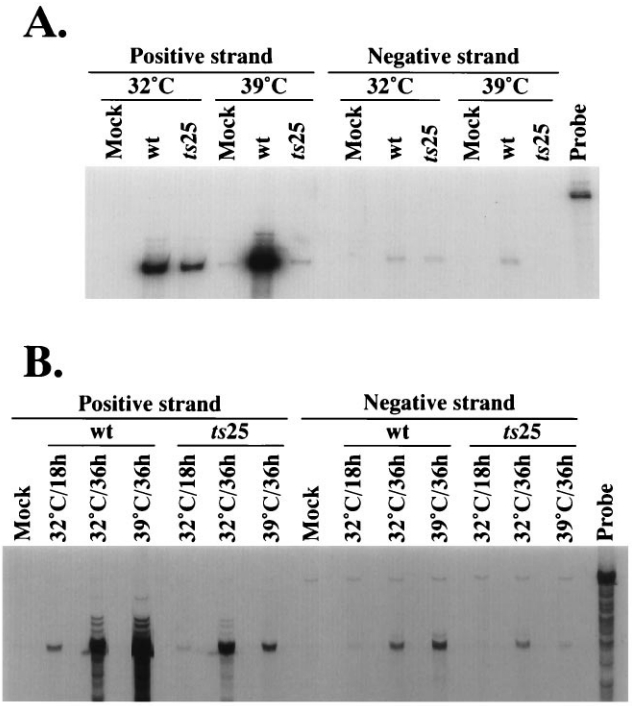

FIG. 3. Accumulation of YFV negative- and positive-strand RNAs. (A) SW-13 monolayers were mock infected or infected at a MOI of 5 PFU of either the wild-type virus (wt) or *ts*25 per cell and incubated at 32 or 39°C for 36 h. Cytoplasmic RNAs were isolated, and the levels of positive- and negative-strand viral RNAs were determined by an RNase protection assay, as described in Materials and Methods. (B) As described for panel A, three sets of SW-13 monolayers were mock infected or infected and incubated at 32°C. RNAs were harvested after 18 h at 32°C or after an additional 18-h incubation at either 32 or 39°C. The sizes of the probe and protected fragments are 284 and 251 nt, respectively. The experiment has been repeated four times with similar results.

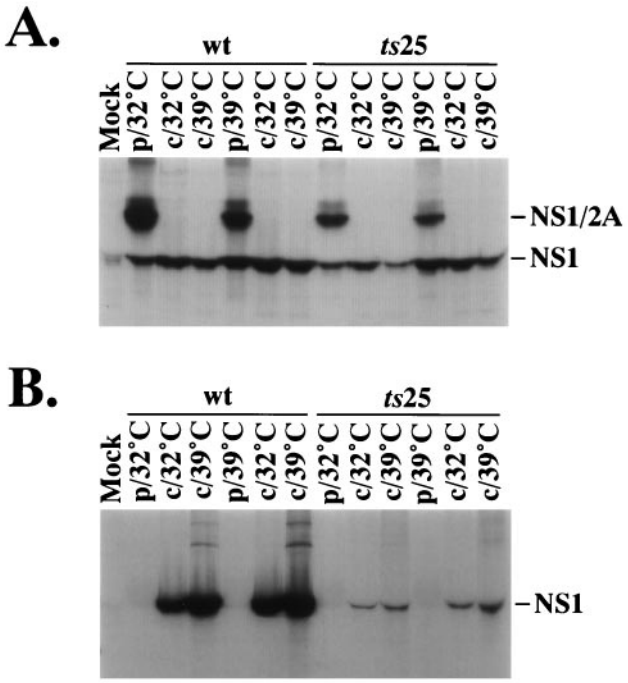

FIG. 4. Effects of temperature on NS1 accumulation, stability, and secretion. SW-13 cells were mock infected or infected at a MOI of 5 PFU of either the wild-type virus (wt) or *ts*25 per cell. After 35 h at 32°C, cells were pulse-labeled (p) for 1 h at either 32 or 39°C and chased (c) for 6 h at either 32 or 39°C. Equivalent portions of SDS-treated cell extracts (A) or culture supernatants (B) were immunoprecipitated with NS1-specific polyclonal and monoclonal antibodies and analyzed by SDS-PAGE (10% polyacrylamide). To allow better visualization of the low levels of NS1 secreted by *ts*25, the autoradiograph shown in panel B was exposed 2.5 times longer than that shown in panel A.

sion has been verified by showing that [^{3}H]uridine can be incorporated into viral genomic RNA after the shift to the nonpermissive temperature (data not shown). Although further experiments are needed, the simplest interpretation of these data is that the *ts*25 lesion inhibits the formation of new RNA replication complexes synthesizing negative- and perhaps positive-strand RNAs (see Discussion).

Effects of the *ts*25 lesion on polyprotein processing and NS1 secretion. The *ts*25 lesion might inhibit the formation or function of YFV RNA replication complexes by affecting YFV polyprotein processing. An octapeptide sequence at the C terminus of NS1 (18) as well as NS2A (16) sequences appears to be important for proper processing at the NS1/2A cleavage site, implying the presence of a functional linkage between these two proteins, which are initially produced as a discrete NS1-2A precursor (6). Cleavages at the 2A/2B site (9) and at an internal cleavage in NS2A (6, 7, 33) are mediated by the flavivirus NS2B-3 serine proteinase. Thus, mutations in NS1 which affect its interaction with NS2A could, in theory, affect processing at downstream sites, which is important for the assembly of functional replicases (8, 9, 33). To examine polyprotein processing and stability in *ts*25-infected cells, infection was established at 32°C and at 35 h p.i., cells were pulse-labeled for 1 h at 32°C and either harvested immediately or incubated for an additional 6 h at 32 or 39°C. YFV-specific proteins were immunoprecipitated and separated by SDS-PAGE. As shown in Fig. 2B, no obvious temperature-dependent defects in *ts*25 NS polyprotein processing or product stability were observed, although it was difficult to distinguish between E and NS1 in this analysis.

We therefore examined NS1 processing, stability, and secretion in more detail. Another pulse-chase experiment was conducted, in which pulse-labeling was performed at 32 or 39°C, and equal portions of the cell lysates (Fig. 4A) or supernatants (Fig. 4B) were analyzed by immunoprecipitation with saturating amounts of a mixture of NS1-specific polyclonal and monoclonal antibodies. Overall, we did not observe any temperature-dependent differences in the processing, stability, or secretion of *ts*25 NS1. Examination of Fig. 4A suggests that while *ts*25 makes somewhat reduced levels of NS1-2A and NS1 relative to the parent, NS1-2A processing is unimpaired regardless of whether the proteins were synthesized at 32 or 39°C. For both the parent and *ts*25, lower levels of cell-associated NS1 were observed after chases at 39°C compared to 32°C, but this most probably reflects more efficient secretion of NS1 at the higher temperature. The most striking observation of the experiment was the markedly reduced levels of NS1 present in the supernatant of *ts*25-infected cells (Fig. 4B). Although this could be due to enhanced susceptibility of the mutant NS1 to degradation in the culture supernatant, it seems more likely that a substantial fraction of the NS1 made by *ts*25, at either temperature, is targeted for intracellular degradation and not secreted.

Effects of the *ts*25 lesion on virus release. Since it had been suggested that NS1 might play a role in virus assembly, maturation, or release, we also examined the production of progeny virus in a temperature shift experiment. Since the primary *ts*25 defect is in RNA accumulation, it was again necessary to establish infection at the permissive temperature. At 45 h p.i. at 32°C, the cell cultures were washed extensively and incubated at either 32 or 39°C for an additional 3 h. As shown in Table 2, the yields of parental virus upon the shift to 39°C were similar to those obtained after continued incubation at 32°C and the yields were less than twofold lower for *ts*25. These results suggest that the *ts*25 lesion does not have a dramatic inhibitory effect on virus release, at least when infection is established at the permissive temperature.

Substitution of Ala for Arg-299 is responsible for the *ts* phenotype. Since *ts*25 contains two Ala substitutions, one at Lys-296 and a second at Arg-299, single substitutions were examined to determine whether one or both mutations were required for the *ts* phenotype. As summarized in Table 1, substitution of Lys-296 with Ala led to a virus (A32) which was indistinguishable from the parent, whereas substitution of Arg-299 with Ala resulted in a mutant (A33) with a *ts* phenotype.

DISCUSSION

Characterization of the 28 clustered charged-amino-acid-to-alanine mutants created in this study provides a preliminary genetic map of NS1 functional domains (Fig. 5). Nine mutations which abrogated plaque formation at either temperature

TABLE 2. Effects of temperature shift on virus release[a]

Virus	Titer of infectious virus released from 45 to 48 h p.i. (PFU/ml) at:		Yield ratio (39°C/32°C)
	32°C	39°C	
wt[b]	1.3×10^7	1.5×10^7	1.1
*ts*25	7.5×10^6	4.5×10^6	0.6

[a] SW-13 cells were infected at 32°C at a MOI of 5 PFU/ml. At 45 h p.i., the cells were washed, prewarmed medium was added, and the incubation was continued for 3 h at either 32°C or after a shift to 39°C. Titers were determined by plaque assay on SW-13 cells.

[b] wt, parental virus.

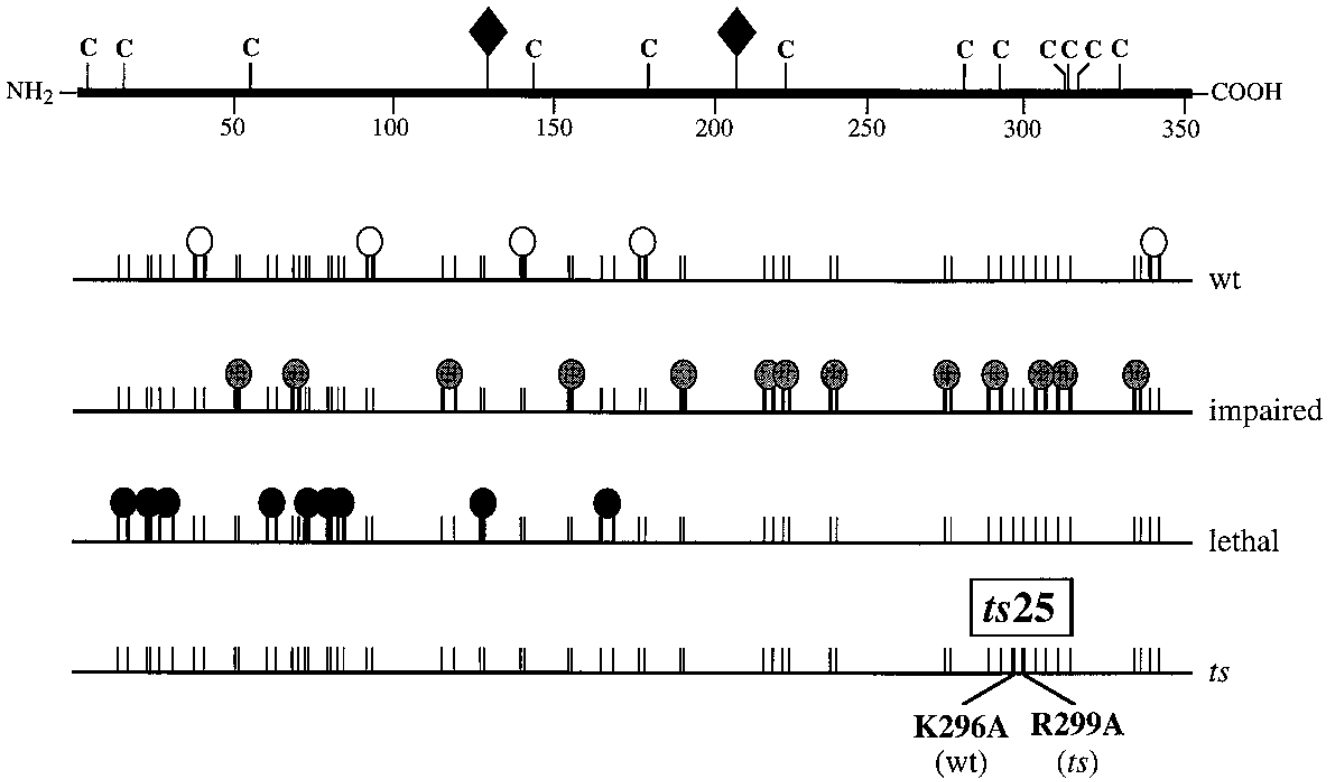

FIG. 5. Summary of NS1 clustered charged-amino-acid-to-alanine mutants. Shown at the top is a schematic of the 352-residue NS1 protein (thick bar) highlighting the conserved Cys residues (C) and N-linked glycosylation sites (◆). Diagrammed below are NS1 mutants grouped by phenotype: wild type (open circles), impaired (shaded circles), lethal (solid circles), or temperature sensitive (*ts*). Details can be found in Table 1 and the text. Vertical lines indicate the positions of charged residues; thicker vertical lines indicate the charged residue(s) mutated to alanine for individual mutants.

were found to be localized in the N-terminal half of NS1. Previous work has shown that ablation of the first (Asn-130) but not the second (Asn-208) N-linked NS1 glycosylation site leads to defects in viral RNA replication, virus production, and pathogenicity (32, 36). Although further genetic, biochemical, and functional studies are needed to confirm this, the N-terminal portion of NS1 may form a separate functional domain. Other mutations, i.e., those leading to an "impaired" or "wild-type" phenotype relative to the parent, were distributed throughout the protein. Substitution of conserved charged residues did not necessarily lead to a mutant phenotype. For instance, the Lys-339 and Glu-342 residues substituted in mutant A29 are conserved among flaviviruses, yet this mutant was similar to the parent in terms of plaque phenotype and growth at 32 and 39°C. In contrast, Asp-27 and Lys-31 are not conserved yet substitution of Ala for these residues in mutant A4 was lethal. It should be pointed out, however, that we have examined plaque phenotype and virus growth at only two temperatures in only a single cell type (human adrenocortical carcinoma SW-13 cells). It will be of interest to conduct more detailed analyses with other cell types, with whole mosquitoes, and with animal pathogenesis models. It is tempting to speculate that substitutions for highly conserved residues, which have minimal effects on RNA replication, may affect other aspects of NS1 function related to its cell surface or secreted forms.

Of the 28 mutants, only *ts*25 was strongly *ts*, and even this mutant was leaky at 39°C, the nonpermissive temperature. Detailed analysis of the *ts*25 phenotype suggested that this lesion leads to an early defect in RNA accumulation which is enhanced at 39°C relative to 32°C, leading to the heat-sensitive phenotype. At the nonpermissive temperature, RNA replication was dramatically delayed relative to that of the parent, but it did occur, as evidenced by the eventual production of virus after prolonged incubation. The resulting progeny were still *ts* and were not likely to be the result of same-site or second-site reversion events. In shift-up experiments, where infection was established at the permissive temperature, negative-strand RNA accumulation was severely impaired whereas significant positive-strand RNA was synthesized, considering the low level of negative-strand template RNA. Although this analysis suggests that the *ts*25 lesion exerts a selective block at negative- versus positive-strand RNA replication complex formation or function, further experiments are needed to confirm this observation. Shift-up experiments failed to provide evidence for a temperature-dependent difference in polyprotein processing or in NS1 stability or secretion. It was clear, however, that significantly less *ts*25 NS1 accumulated in the culture supernatant at either temperature. Barring enhanced susceptibility to degradation in this extracellular compartment, these results suggest that a large fraction of *ts*25 NS1 may be targeted for intracellular degradation and is not secreted.

The temperature sensitivity of *ts*25 correlated with the Ala substitution at Arg-299, which is located in the C-terminal portion of the 352-residue NS1 protein. As shown in Fig. 6, this NS1 residue is conserved among flaviviruses. The second Ala substitution in *ts*25, at Lys-296, produced a mutant phenotypically indistinguishable from the parent. This position is not highly conserved, and in fact, Ala is present at this position in TBE NS1. Although we cannot formally exclude the possibility

```
YF          GRGKSTRSTI
DEN1        N..P.L.T..
DEN2        N..P.L.T..
DEN3        T..P.L.T..
DEN4        H..P.L.T..
JE          K..P.V.T..
KUN         H..PAT.T..
MVE         K..P.V.I..
SLE         N..A.L.T..
WN          H..PAA.T..
TBE         K..A.V....
ts25        ...A..A...
A32 (wt)    ...A......
A33 (ts)    ......A...
```

FIG. 6. Comparison of flavivirus NS1 sequences in the vicinity of the *ts*25 lesion. Shown is an alignment of NS1 residues 293 to 302 (YFV numbering) for 11 different flaviviruses, *ts*25, and single substitution mutants A32 and A33. Positions identical to the YFV sequence are indicated by dots, and the conserved Arg-299 residue is shown in boldface type. Abbreviations: YF, yellow fever virus; DEN1, dengue 1 virus; DEN2, dengue 2 virus; DEN3, dengue 3 virus; DEN4, dengue 4 virus; JE, Japanese encephalitis virus; KUN, Kunjin virus; MVE, Murray Valley encephalitis virus; SLE, St. Louis encephalitis virus; WN, West Nile virus; TBE, tick-borne encephalitis virus. Primary references for these flavivirus sequences can be found in references 5 and 35.

that the nucleotide substitutions creating the Arg-299 substitution are exerting an effect at the RNA level, the simplest interpretation of our results is that substitution of Arg-299 impairs the ability of NS1 to function in some aspect of RNA replication. Other mutagenesis studies also implicate the C-terminal portion of the NS1 as an important functional domain. Substitution mutations in the C-terminal eight residues can have dramatic effects on NS1-2A cleavage efficiency (18). In addition, Ala substitutions for the three conserved Cys residues near the C terminus of DEN2 NS1 resulted in destabilization of dimers and inhibition of secretion (37).

At present, the role which NS1 plays in RNA replication is not clear; several non-mutually exclusive models can be envisioned. NS1 could play a direct role in replicase function. It seems unlikely, however, that NS1 has an enzymatic activity required for RNA amplification, given its luminal localization. Rather, NS1 might be a structural component of RNA replication complexes via direct interaction with other membrane-spanning or membrane-associated viral or host components. Alternatively, NS1 may not be present in functioning replicases but may be required for an early step in replication complex assembly. In this regard, RNA replication for positive-strand RNA viruses occurs in association with cellular membranes; significant proliferation and reorganization of membrane organelles is often associated with virus infection. In poliovirus, such changes can be triggered by specific viral proteins (2, 10, 14). Furthermore, the inhibition of poliovirus RNA replication by brefeldin A suggests that some portion of the secretory apparatus is required for the assembly of functional replication complexes (13, 30). Given this precedent, NS1 might facilitate the formation of membrane organelles required for the assembly of functional flavivirus RNA replication complexes or target replicase components to the proper subcellular compartment. The *ts*25 lesion could either directly interfere with NS1 function and/or lead to limiting quantities of functional NS1 via destabilization and turnover of the protein. Either model could explain the observed *ts*25 RNA phenotype. At 32°C, lower levels of functional NS1 would lead to a slight delay in achieving saturating levels of negative- and positive-strand RNA replication complexes. At 39°C, the NS1 defect is more severe, leading to extremely slow RNA replication complex formation and RNA accumulation, delayed virus production, minimal CPE, and no plaque formation. Shift-up experiments, which suggest a selective block in negative-strand RNA accumulation, may indicate that NS1 is no longer required once a functional positive-strand replication complex has been formed.

Although a role for NS1 in virion morphogenesis or release was previously proposed, no data have been obtained to support this. In our study, shift-up experiments with *ts*25 did not demonstrate a significant defect in the release of infectious virus. Furthermore, at both 32 and 39°C, the secretion of *ts*25 NS1 appeared to be severely impaired. Thus, in mammalian cells, successful transit of NS1 through the secretory pathway is not linked to virus release. This is also true for mosquito cells, which do not secrete NS1 but are highly permissive for flavivirus RNA replication and production of infectious virus (29). These results, which implicate NS1 in flavivirus RNA replication but not virion production, are consistent with a recent immunolocalization study (28). DEN2 NS1 was shown to be associated with intracellular membrane organelles and colocalized with other nonstructural replicase components including double-stranded RNA. NS1 did not colocalize with vesicles containing DEN2 structural proteins and intracellular virus particles.

In summary, our study provides strong evidence that NS1 is required for an early step in flavivirus RNA replication. Additional work is needed to define its precise role in RNA replication complex assembly and/or function. Further analysis of *ts*25 as well as the other clustered charged-amino-acid-to-alanine NS1 mutants may help to elucidate related or distinct functions for NS1 in flavivirus replication and pathogenesis.

ACKNOWLEDGMENTS

We thank Sean M. Amberg and Brett D. Lindenbach for critical reading of the manuscript and for helpful comments.

I.R.M. was supported by a fellowship from Capes/CNPq and PHS grant AI31501 to C.M.R. R.G. acknowledges support from the Rockefeller Foundation (Biotechnology Career Program) and CNPq.

REFERENCES

1. **Ausubel, F. M., R. Brent, R. E. Kingston, D. D. Moore, J. G. Seidman, J. A. Smith, and K. Struhl (ed.).** 1993. Current protocols in molecular biology. Greene Publishing Associates, New York, N.Y.
2. **Barco, A., and L. Carrasco.** 1995. A human virus protein, poliovirus protein 2BC, induces membrane proliferation and blocks the exocytic pathway in the yeast *Saccharomyces cerevisiae*. EMBO J. **14:**3349–3364.
3. **Brinton, M. A.** 1986. Replication of flaviviruses, p. 327–365. *In* S. Schlesinger and M. J. Schlesinger (ed.), The Togaviridae and Flaviviridae. Plenum Press, New York, N.Y.
4. **Chamberlain, J. P.** 1979. Fluorographic detection of radioactivity in polyacrylamide gels with the water-soluble fluor, sodium salicylate. Anal. Biochem. **98:**132–135.
5. **Chambers, T. J., C. S. Hahn, R. Galler, and C. M. Rice.** 1990. Flavivirus genome organization, expression, and replication. Annu. Rev. Microbiol. **44:**649–688.
6. **Chambers, T. J., D. W. McCourt, and C. M. Rice.** 1990. Production of yellow fever virus proteins in infected cells: identification of discrete polyprotein species and analysis of cleavage kinetics using region-specific polyclonal antisera. Virology **177:**159–174.
7. **Chambers, T. J., D. W. McCourt, and C. M. Rice.** 1989. Yellow fever virus proteins NS2A, NS2B, and NS4B: identification and partial N-terminal amino acid sequence analysis. Virology **169:**100–109.
8. **Chambers, T. J., A. Nestorowicz, and C. M. Rice.** 1995. Mutagenesis of the yellow fever virus NS2B/3 cleavage site: determinants of cleavage site specificity and effects on polyprotein processing and viral replication. J. Virol. **69:**1600–1605.
9. **Chambers, T. J., R. C. Weir, A. Grakoui, D. W. McCourt, J. F. Bazan, R. J. Fletterick, and C. M. Rice.** 1990. Evidence that the N-terminal domain of nonstructural protein NS3 from yellow fever virus is a serine protease responsible for site-specific cleavages in the viral polyprotein. Proc. Natl. Acad. Sci. USA **87:**8898–8902.
10. **Cho, M. W., N. Teterina, D. Egger, K. Bienz, and E. Ehrenfeld.** 1994. Membrane rearrangement and vesicle induction by recombinant poliovirus 2C and 2BC in human cells. Virology **202:**129–145.
11. **Collett, M. S.** Personal communication.
12. **Diamond, S. E., and K. Kirkegaard.** 1994. Clustered charged-to-alanine mutagenesis of poliovirus RNA-dependent RNA polymerase yields multiple

temperature-sensitive mutants defective in RNA synthesis. J. Virol. **68:**863–876.
13. **Doedens, J., L. A. Maynell, M. W. Klymkowsky, and K. Kirkegaard.** 1994. Secretory pathway function, but not cytoskeletal integrity, is required in poliovirus infection. Arch. Virol. Suppl. **9:**159–172.
14. **Echeverri, A. C., and A. Dasgupta.** 1995. Amino terminal regions of poliovirus 2C protein mediate membrane binding. Virology **208:**540–553.
15. **Eckels, K. H., P. L. Summers, and P. K. Russell.** 1983. Temperature-sensitive events during the replication of the attenuated S-1 clone of dengue type 2 virus. Infect. Immun. **39:**750–754.
16. **Falgout, B., R. Chanock, and C.-J. Lai.** 1989. Proper processing of dengue virus nonstructural glycoprotein NS1 requires the N-terminal hydrophobic signal sequence and the downstream nonstructural protein NS2a. J. Virol. **63:**1852–1860.
17. **Gould, E. A., A. Buckley, A. D. T. Barrett, and N. Cammack.** 1986. Neutralizing (54K) and non-neutralizing (54K and 48K) monoclonal antibodies against structural and nonstructural yellow fever virus proteins confer immunity in mice. J. Gen. Virol. **67:**591–595.
18. **Hori, H., and C.-J. Lai.** 1990. Cleavage of dengue virus NS1-NS2A requires an octapeptide sequence at the C terminus of NS1. J. Virol. **64:**4573–4577.
19. **Jacobs, S. C., J. R. Stephenson, and G. W. Wilkinson.** 1992. High-level expression of the tick-borne encephalitis virus NS1 protein by using an adenovirus-based vector: protection elicited in a murine model. J. Virol. **66:**2086–2095.
20. **Jacobs, S. C., J. R. Stephenson, and G. W. Wilkinson.** 1994. Protection elicited by a replication-defective adenovirus vector expressing the tick-borne encephalitis virus nonstructural glycoprotein NS1. J. Gen. Virol. **75:** 2399–2402.
21. **Kamer, G., and P. Argos.** 1984. Primary structural comparison of RNA-dependent polymerases from plant, animal, and bacterial viruses. Nucleic Acids Res. **12:**7269–7282.
22. **Kapoor, M., L. Zhang, M. Ramachandra, J. Kusukawa, K. E. Ebner, and R. Padmanabhan.** 1995. Association between NS3 and NS5 proteins of dengue virus type 2 in the putative RNA replicase is linked to differential phosphorylation of NS5. J. Biol. Chem. **270:**19100–19106.
23. **Koonin, E. V.** 1993. Computer-assisted identification of a putative methyltransferase domain in NS5 protein of flaviviruses and lambda 2 protein of reovirus. J. Gen. Virol. **74:**733–740.
24. **Kunkel, T. A.** 1985. Rapid and efficient site-specific mutagenesis without phenotypic selection. Proc. Natl. Acad. Sci. USA **82:**488–492.
25. **Laemmli, U. K.** 1970. Cleavage of structural proteins during the assembly of the head of bacteriophage T4. Nature (London) **227:**680–685.
26. **Lin, C., S. M. Amberg, T. J. Chambers, and C. M. Rice.** 1993. Cleavage at a novel site in the NS4A region by the yellow fever virus NS2B-3 proteinase is a prerequisite for processing at the downstream 4A/4B signalase site. J. Virol. **67:**2327–2335.
27. **Lin, C., T. J. Chambers, and C. M. Rice.** 1993. Mutagenesis of conserved residues at the yellow fever virus 3/4A and 4B/5 dibasic cleavage sites: effects on cleavage efficiency and polyprotein processing. Virology **192:**596–604.
28. **Mackenzie, J. M., M. K. Jones, and P. R. Young.** 1996. Immunolocalization of the dengue virus nonstructural glycoprotein NS1 suggests a role in viral RNA replication. Virology **220:**232–240.
29. **Mason, P. W.** 1989. Maturation of Japanese encephalitis virus glycoproteins produced by infected mammalian and mosquito cells. Virology **169:**354–364.
30. **Maynell, L. A., K. Kirkegaard, and M. W. Klymkowsky.** 1992. Inhibition of poliovirus RNA synthesis by brefeldin A. J. Virol. **66:**1985–1994.
31. **Monath, T. P., and F. X. Heinz.** 1996. Flaviviruses, p. 961–1034. *In* B. N. Fields, D. M. Knipe, and P. M. Howley (ed.), Fields virology, 3rd ed. Raven Press, New York, N.Y.
32. **Muylaert, I. R., R. G. Galler, and C. M. Rice.** 1996. Mutagenesis of the N-linked glycosylation sites of the yellow fever virus NS1 protein: effects on virus replication and mouse neurovirulence. Virology, **222:**159–168.
33. **Nestorowicz, A., T. J. Chambers, and C. M. Rice.** 1994. Mutagenesis of the yellow fever virus NS2A/2B cleavage site: effects on proteolytic processing, viral replication and evidence for alternative processing of the NS2A protein. Virology **199:**114–123.
34. **Novak, J. E., and K. Kirkegaard.** 1991. Improved method for detecting poliovirus negative strands used to demonstrate specificity of positive-strand encapsidation and the ratio of positive to negative strands in infected cells. J. Virol. **65:**3384–3387.
35. **Osatomi, K., and H. Sumiyoshi.** 1990. Complete nucleotide sequence of dengue type 3 virus genome RNA. Virology **176:**643–647.
36. **Pletnev, A. G., M. Bray, and C. J. Lai.** 1993. Chimeric tick-borne encephalitis and dengue type 4 viruses: effects of mutations on neurovirulence in mice. J. Virol. **67:**4956–4963.
37. **Pryor, M. J., and P. J. Wright.** 1993. The effects of site-directed mutagenesis on the dimerization and secretion of the NS1 protein specified by dengue virus. Virology **194:**769–780.
38. **Rice, C. M.** 1996. *Flaviviridae*: the viruses and their replication, p. 931–960. *In* B. N. Fields, D. M. Knipe, and P. M. Howley (ed.), Fields virology, 3rd ed. Raven Press, New York, N.Y.
39. **Rice, C. M., A. Grakoui, R. Galler, and T. J. Chambers.** 1989. Transcription of infectious yellow fever virus RNA from full-length cDNA templates produced by in vitro ligation. New Biol. **1:**285–296.
40. **Rice, C. M., E. M. Lenches, S. R. Eddy, S. J. Shin, R. L. Sheets, and J. H. Strauss.** 1985. Nucleotide sequence of yellow fever virus: implications for flavivirus gene expression and evolution. Science **229:**726–733.
41. **Rice, C. M., E. G. Strauss, and J. H. Strauss.** 1986. Structure of the flavivirus genome, p. 279–326. *In* S. Schlesinger and M. J. Schlesinger (ed.), The Togaviridae and Flaviviridae. Plenum Press, New York, N.Y.
42. **Rice, C. M., and J. H. Strauss.** 1990. Production of flavivirus polypeptides by proteolytic processing. Semin. Virol. **1:**357–367.
43. **Sambrook, J., E. Fritsch, and T. Maniatis.** 1989. Molecular cloning: a laboratory manual. Cold Spring Harbor Laboratory, Cold Spring Harbor, N.Y.
44. **Schlesinger, J. J., M. W. Brandriss, C. B. Cropp, and T. P. Monath.** 1986. Protection against yellow fever in monkeys by immunization with yellow fever virus nonstructural protein NS1. J. Virol. **60:**1153–1155.
45. **Schlesinger, J. J., M. W. Brandriss, and T. P. Monath.** 1983. Monoclonal antibodies distinguish between wild and vaccine strains of yellow fever virus by neutralization, hemagglutination inhibition, and immune precipitation of the virus envelope protein. Virology **125:**8–17.
46. **Schlesinger, J. J., M. W. Brandriss, and E. E. Walsh.** 1985. Protection against 17D yellow fever encephalitis in mice by passive transfer of monoclonal antibodies to the nonstructural glycoprotein gp48 and by active immunization with gp48. J. Immunol. **135:**2805–2809.
47. **Schlesinger, J. J., M. Foltzer, and S. Chapman.** 1993. The Fc portion of antibody to yellow fever virus NS1 is a determinant of protection against YF encephalitis in mice. Virology **192:**132–141.
48. **Tan, B.-T., J. Fu, R. J. Sugrue, E.-H. Yap, Y.-C. Chan, and Y. H. Tan.** 1996. Recombinant dengue type 1 virus NS5 protein expressed in *Escherichia coli* exhibits RNA-dependent RNA polymerase activity. Virology **216:**317–325.
49. **Warrener, P., J. K. Tamura, and M. S. Collett.** 1993. An RNA-stimulated NTPase activity associated with yellow fever virus NS3 protein expressed in bacteria. J. Virol. **67:**989–996.
50. **Wengler, G., and G. Wengler.** 1993. The NS 3 nonstructural protein of flaviviruses contains an RNA triphosphatase activity. Virology **197:**265–273.
51. **Wertman, K. F., D. G. Drubin, and D. Botstein.** 1992. Systematic mutational analysis of the yeast *ACT1* gene. Genetics **132:**337–350.
52. **Westaway, E. G.** 1987. Flavivirus replication strategy. Adv. Virus Res. **33:** 45–90.
53. **Winkler, G., S. E. Maxwell, C. Ruemmler, and V. Stollar.** 1989. Newly synthesized dengue-2 virus nonstructural protein NS1 is a soluble protein but becomes partially hydrophobic and membrane-associated after dimerization. Virology **171:**302–305.
54. **Winkler, G., V. B. Randolph, G. R. Cleaves, T. E. Ryan, and V. Stollar.** 1988. Evidence that the mature form of the flavivirus nonstructural protein NS1 is a dimer. Virology **162:**187–196.